

---

# APDL IMPLEMENTATION OF A 3D FEM CAPACITANCE SIMULATOR FOR ARBITRARILY SHAPED INTERCONNECTS

---

A. Hieke<sup>†</sup>

SIEMENS Microelectronics, c/o IBM Semiconductor Research & Development Center (DRAM Development Alliance), Hopewell Junction, NY 12533, U.S.A.

## Abstract

This paper describes the implementation of an ANSYS<sup>TM</sup> Parametric Design Language (APDL) macro called CAMACO for the computation of capacitance matrixes of arbitrarily shaped 3D objects in arbitrarily distributed dielectrics via the conservation of field energies. The most significant advantage is the utilization of the advanced 3D capabilities of ANSYS<sup>TM</sup> to generate, edit and visualize realistically shaped ('non-Manhattan') 3D structures either by parametric description and/or graphical interaction (e.g. spaceball; VRML models etc.) exceeding known solution. These features are especially helpful for initial principal design studies on potential structures of MEMS, ULSI, MCMs, etc. requiring precise capacitances computations of arbitrarily shaped 3D objects.

**Keywords:** capacitance simulation, 3D FEM, interconnect, ANSYS, APDL, CAMACO, MEMS, realistically shaped

---

## 1. Introduction

The exact computation of electric capacitances of interconnects within integrated structures especially deep sub-micron ULSI, MEMS and other microsystems has become a crucial part of design and performance prediction. A variety of numerical methods and algorithms for the computation of electrostatic field problems and the subsequent calculation of capacitances of 2D and 3D geometries have been repeatedly reported in the past. Most papers put emphasis on efficient and accelerated numerical algorithms, e.g. [21,25,26,34,44,46,55, 58].

Several programs are known which can compute mutual capacitances. However, most of them provide limited capabilities in terms of fast interactive 3D model generation and visualization. Furthermore the simulation of realistically smooth-shaped objects is rarely possible. However, the realistic representation of interconnects is essential for high precision capacitance computations.

Since complexity significantly increases with the step from 2D to 3D models, a potential user is no longer able to imagine the whole model or draw a complete sketch from which an input-file for a simulator could be written. As a result, the demands on a true 3D capacitance simulation program exceed the pure capability to solve electrostatic field problems correct and fast but also include an user-interface for interactive model design and model data base management. These demands represent an effort of several man-years if implemented in classical high level languages. A solution to this problem is provided by implementing CAMCAO as an APDL macro.

## 2. Theoretical Background

### 2.1. History

Early works on numerical capacitance computation from Reitan/ Higgins date back as far as 1951 [1,2]. Further developments with practical applications were then primarily initiated by the microwave community and later by demands for increased speed and performance of VLSI / ULSI and printed circuit boards as numerous publications starting about 1970 until this day indicate [3-60].

The interested reader is furthermore referred to a variety of books about theoretical electrodynamics [61-74] (1953-1998) which all more or less detailed explain the subsequent outlined principle of mutual capacitance, partially with some remarks on numerical implementation. As further source for some insight into the matter the manuals and user guides to the mentioned programs are recommended [75-85].

### 2.2. Physical Aspects

A pure electrostatic system is governed by the Maxwell equation

$$\iiint_v \rho dV = \epsilon_r \epsilon_0 \oint \vec{E}(\vec{r}) d\vec{A} \quad (1)$$

(Gauss's law) and the derivable Poisson equation

$$\epsilon_0 \nabla[(\epsilon_r(\vec{r}) \nabla \varphi(\vec{r}))] = -\rho(\vec{r}) \quad (2)$$

For the given problem, dielectrics may be distributed arbitrarily but no space charge effects apply. In a system of  $n$

---

<sup>†</sup>v2hieke@us.ibm.com;ahi@ieee.org

conductors the charge  $Q_i$  on each conductor  $i$  for a given set of boundary conditions can be calculated by means of the capacitance matrix

$$Q_i = \sum_{j=1, j \neq i}^n C_{ij} U_{ij} \quad (3)$$

taking into account the voltage difference  $U_{ij}$  between each conductor  $i$  and the remaining  $(n-1)$  conductors. Due to this definition and the physical nature of the problem the coefficients,  $C_{ij}$ , follow three restrictions: The matrix is (I) square, (II) symmetrical and (III) the diagonal elements are equal to the sum over the remaining elements in a line

$$C_{ii} = - \sum_{j=1, j \neq i}^n C_{ij} \quad (4)$$

Therefore the number of unknown values is

$$n_{cap} = \frac{n(n-1)}{2} \quad (5)$$

These values represent the mutual capacitances while the  $C_{ii}$  represent the derivable self capacitance values. To calculate the charge on a conductor one could use Eq. (1) and integrate the electrical field over the closed surface of each conductor

$$Q_i = \epsilon_r \epsilon_0 \oint \vec{E}(\vec{r}) d\vec{A} \quad (6)$$

usually referred to as principle of charge conservation. However, for numerical reasons a far more accurate and computationally simpler way is to apply the principle of energy conservation using the electric field energy stored in the volume  $V$  of a given field configuration and determined by the boundary conditions:

$$W = \frac{1}{2} \epsilon_0 \iiint_V \epsilon_r(\vec{r}) [\nabla \phi(\vec{r})]^2 dV \quad (7)$$

which can be simplified by recognizing that

$$W = \frac{1}{2} \epsilon_0 \iiint_V \epsilon_r(\vec{r}) [\vec{E}(\vec{r})]^2 dV \quad (8)$$

which simplifies to

$$W = \frac{1}{2} \iiint_V \vec{E}(\vec{r}) \vec{D}(\vec{r}) dV. \quad (9)$$

The Equations (7)-(9) apply in general to arbitrarily distributed dielectrics. Furthermore, the relation

$$W = \frac{1}{2} C U^2 \quad (10)$$

is used to set up a linear system of equations with  $n_{cap}$  unknowns containing the squares of the voltage differences  $1/2 \cdot k U_{ij}^2$  and the respective field energies,  $W_k$ ,

$$\begin{bmatrix} \frac{1}{2} U_{12}^2 & \frac{1}{2} U_{13}^2 & \frac{1}{2} U_{14}^2 & \frac{1}{2} U_{23}^2 & \frac{1}{2} U_{24}^2 & \frac{1}{2} U_{34}^2 \\ \frac{1}{2} U_{12}^2 & \frac{1}{2} U_{13}^2 & \frac{1}{2} U_{14}^2 & \frac{1}{2} U_{23}^2 & \frac{1}{2} U_{24}^2 & \frac{1}{2} U_{34}^2 \\ \vdots & \vdots & \vdots & \vdots & \vdots & \vdots \\ \frac{1}{2} U_{12}^2 & \frac{1}{2} U_{13}^2 & \frac{1}{2} U_{14}^2 & \frac{1}{2} U_{23}^2 & \frac{1}{2} U_{24}^2 & \frac{1}{2} U_{34}^2 \end{bmatrix} \begin{bmatrix} C_{12} \\ C_{13} \\ C_{14} \\ C_{23} \\ C_{24} \\ C_{25} \end{bmatrix} = \begin{bmatrix} W_1 \\ W_2 \\ W_3 \\ W_4 \\ W_5 \\ W_6 \end{bmatrix} \quad (11)$$

here exemplified for a 4-body system with 6 unknowns. A set of  $k = 1 \dots n_{cap}$  linear independent vectors containing the squares of the voltage differences  $1/2 \cdot k U_{ij}^2$  has to be created ensuring that the determinant of the resulting matrix is non-zero. The  $n_{cap}$  energies  $W_k$  of the respective field distributions are the quantities to be calculated.

It was found, that the following simple algorithm, subsequently given in APDL notation, meets these requirements:

```

nun=nbody*(nbody-1)/2
uset=0
*do,i,1,nbody
    uset=uset+1
    U(uset,i)=voltage
*enddo
k=0
*do,i,1,nun
    *do,l,i+1,nbody-1
        uset=uset+1
        *if,uset,gt,nun,exit
        *do,k,1,i
            U(uset,k)=voltage
        *enddo
        U(uset,l)=voltage
    *enddo
    *if,uset,gt,nun,exit
*enddo

```

The algorithm generates sets of Dirichlet boundary conditions  $U(n_{cap}, n)$  as illustrated for the case of 7 bodies in Table 1.

However, it is not necessary to obtain  $n_{cap}$  field solution (21 for this example) but only  $n$  field solutions, thus dramatically reducing the numerical effort for large numbers of  $n$ . This is accomplished using the linear nature of the problem and generating all necessary  $n_{cap}$  solution by superposition of solutions obtained from  $n$  linear independent boundary condition vectors; for practical purposes the first  $n$  from the

scheme above [17,60,75].

Table 1: Dirichlet boundary condition scheme  $U(n_{cap}, n)$  for a 7-body problem; (1 = voltage on; 0 = voltage off)

<b>k</b>	<b><math>U(k,1)</math></b>	<b><math>U(k,2)</math></b>	<b><math>U(k,3)</math></b>	<b><math>U(k,4)</math></b>	<b><math>U(k,5)</math></b>	<b><math>U(k,6)</math></b>	<b><math>U(k,7)</math></b>
1	1	0	0	0	0	0	0
2	0	1	0	0	0	0	0
3	0	0	1	0	0	0	0
4	0	0	0	1	0	0	0
5	0	0	0	0	1	0	0
6	0	0	0	0	0	1	0
7	0	0	0	0	0	0	1
8	1	1	0	0	0	0	0
9	1	0	1	0	0	0	0
10	1	0	0	1	0	0	0
11	1	0	0	0	1	0	0
12	1	0	0	0	0	1	0
13	1	1	1	0	0	0	0
14	1	1	0	1	0	0	0
15	1	1	0	0	1	0	0
16	1	1	0	0	0	1	0
17	1	1	1	1	0	0	0
18	1	1	1	0	1	0	0
19	1	1	1	0	0	1	0
20	1	1	1	1	1	0	0
21	1	1	1	1	0	1	0

In general it would be sufficient to store only the potential distributions  $\phi(\vec{r})$  and obtain the  $\vec{E}(\vec{r})$  and  $\vec{D}(\vec{r})$  field after the superposition. However this approach, while low in its memory requirements, faces two problems:

1. In order to get  $\vec{D}(\vec{r})$  from a  $\phi(\vec{r})$  solution obtained by superposition, one needs to know  $\epsilon_r(\vec{r})$  which may be in general arbitrarily distributed in the considered volume. The geometry is described by means of objects (e.g. layers) with certain properties including  $\epsilon_r$  and it would be too time consuming to retrieve this information.
2. ANSYS<sup>TM</sup> has no intrinsic single command gradient function applicable to a user-generated scalar field. An additional implementation would be too time consuming.

Consequently, the  $\vec{E}(\vec{r})$  and  $\vec{D}(\vec{r})$  fields are stored and not  $\phi(\vec{r})$ . The macro initially generates an array  $U(n_{cap}, n)$  which is filled by the above mentioned algorithm with  $n_{cap}$  sets of boundary conditions for all  $n$  bodies as for example shown in Table 1. The Laplace problem is solved  $n$  times with the first  $n$  boundary condition sets. The fields  $\vec{E}(\vec{r})$  and  $\vec{D}(\vec{r})$  from these  $n$  solutions are stored in 6 arrays:

$$E_x(n, n_{element\_max}), E_y(n, n_{element\_max}), E_z(n, n_{element\_max})$$

$$D_x(n, n_{element\_max}), D_y(n, n_{element\_max}), D_z(n, n_{element\_max})$$

for all  $n$  field solutions and all  $n_{element\_max}$  elements of the model. A further vector, containing the volumes of all elements  $V_{elem}(n_{element\_max})$  is generated. Next the matrix of voltage differences and the vector of field energies can be assembled according to (11) with the actual number of  $n_{cap}$ .

The matrix of voltage differences is easily created by using the before mentioned array  $U(n_{cap}, n)$  of Dirichlet boundary condition. The same array is used to determine which of the first  $n$  solutions are needed for the subsequent computation of the field energies and the filling of the field energy vector  $W_k$  in order to solve (11). The first  $k = 1 \dots n$  field energy values are obtained by

$$W_k = \frac{1}{2} \sum_{l=1}^{n_{element\_max}} \sqrt{E_x k, l^2 + E_y k, l^2 + E_z k, l^2} \\ \cdot \sqrt{D_x k, l^2 + D_y k, l^2 + D_z k, l^2} \cdot V_{elem l} \quad (12)$$

and the remaining  $k = (n+1) \dots n_{cap}$  solutions require superposition

$$W_k = \frac{1}{2} \sum_{l=1}^{n_{element\_max}} \sqrt{\left[ \sum_{\forall U(l \neq 0)}^n E_x k, l \right]^2 + \left[ \sum_{\forall U(l \neq 0)}^n E_y k, l \right]^2 + \left[ \sum_{\forall U(l \neq 0)}^n E_z k, l \right]^2} \\ \cdot \sqrt{\left[ \sum_{\forall U(l \neq 0)}^n D_x k, l \right]^2 + \left[ \sum_{\forall U(l \neq 0)}^n D_y k, l \right]^2 + \left[ \sum_{\forall U(l \neq 0)}^n D_z k, l \right]^2} \cdot V_{elem l} \quad (13)$$

Equation (11), according to the actual number of unknowns, is solved and the capacitance matrix  $C_{ij}$  is filled by obtaining the  $C_{ii}$  via (4) and using the symmetry condition.

It may be expected that the results do slightly depend on the order in which the bodies are numbered especially in cases with high physical asymmetry because the capacitance matrix is derived from a selected group of boundary condition sets. In general, this group will not represent the numerically best suited cases out of all possible boundary conditions sets. No investigations have been made in this direction since it is most likely that this effect is smaller than the errors due to discretization. Furthermore it is difficult to avoid and the influence may also be estimated by changing the numbering of the bodies.

### 3. Some Remarks on the Implementation and Execution

#### 3.1. ANSYS<sup>TM</sup> and APDL

The primary reason for implementing the before described algorithm for the computation of capacitance matrixes in APDL was the high level of abstraction this language provides in comparison with ordinary languages like C, FORTRAN or BASIC. This was the condition to be able to create a software tool like this with significantly reduced effort.

The reader has to be referred at least to the set of standard manual [80-83] from ANSYS<sup>TM</sup> if a deeper understanding of the functionality is required. A potential user of the system must be aware of the model generation principles of ANSYS<sup>TM</sup>. It is his responsibility to describe, create and mesh the model, which is in general more complicated than what usually capacitance simulation programs like

RAPHAEL<sup>TM</sup> (TMA/Avant!), SOLIDIS<sup>TM</sup> (ISE) or CLEVER<sup>TM</sup> (Silvaco) demand. However, if familiar with the ANSYS<sup>TM</sup> environment and language a user has powerful possibilities to create and edit complicated 3D models, beyond known programs or as the later discussed simple examples may imply. It is e.g. possible, to create smooth shapes with splines, skinning these splines to volumes, extruding arbitrary areas along paths etc. as the application in the later discussed 1 Gbit DRAM cell analysis shows. Different CAD file formats can be read; structures and results can be written in VRML format. It would exceed the scope of this paper to go into this matter in detail.

Two version of CAMACO for 2D and 3D problems exist. User input (from an input script or command line) is a sequence of commands that defines the number of bodies (volumes or areas) and their reference number which will then be considered as the bodies for which the capacitance matrix has to be calculated. This information is used by CAMACO to determine matrix sizes, boundary conditions etc. No restrictions about the number or distribution of dielectrics exist. If CAMACO has been stored as \*.mac files in the appropriate path it becomes generally known as a new command.

Since ANSYS<sup>TM</sup> can operate with very complicated material properties it would theoretically be possible to define nonlinear dielectrics and nonisotropic properties. This might be applicable without too many problems to two-body problems. However, significant ramifications must be assumed for multi-body systems, possibly invalidating the simple definition of the capacitance matrix. No further investigations or tests have been made in this direction.

### 3.2. Hardware requirements

The CAMACO/ANSYS<sup>TM</sup> results presented in the next section have been obtained from jobs running on a Dual PentiumII 400 MHz machine with 1024 Mbyte RAM<sup>†</sup>, an Intergraph Intense 3Dpro3410GT video system and a Spaceball 3003 (Spacetec IMC Corporation) as 6-axis input device under WindowsNT 4.0.

The most important requirements on a machine to run ANSYS<sup>TM</sup> jobs with resolutions necessary for realistically shaped 3D objects is RAM. For models with some  $10^5$  nodes at least 512 Mbyte are recommended. These memory requirements to solve a system of  $n$  unknowns may appear high in comparison with an iterative FDM solver but as demonstrated later, results of a given precision can be

<sup>†</sup>Formerly the PentiumII CPU has been incapable of caching more than 512MB RAM. A system equipped with more memory would have suffered a significant performance drop. However, as not generally known PentiumII CPUs with a core stepping "dA1" or later can cache the whole addressable range. The author is not aware of a method to read out the core stepping by means of any program (the stepping can be read out). The only possibility is to locate the SL-sSpec number (e.g. "SL2SH") on the case of the CPU and retrieve the corresponding core stepping date from [86]. (PentiumIII and ATHLON CPUs can cache the whole addressable range)

obtained with significantly fewer unknowns. Secondly, a high end OpenGL hardware accelerated video system is required in order to take advantage of the interactive model creation possibilities.

Among the variety of provided ANSYS<sup>TM</sup> solvers the Preconditioned Conjugate Gradient solver has been used due to its speed; single electrostatic 3D problems with  $10^6$  unknowns have been solved in less than 1hour.

The RAPHAEL<sup>TM</sup> (batch) jobs, which served to obtain reference results, have been executed on an IBM RS/6000 591 (77 Mhz Power2 CPU) with 1.5 Gbyte RAM under AIX 4.2.0.

## 4. Computational Results

### 4.1. Motivation

It is generally complicated to determine the precision of results from multi-body capacitance simulations. The systematic evaluation of the numerical behavior remains crucial to establish a trustworthy tool. Only few cases with analytical solution for the capacitance of two conductors are known. More complicated models can only be judged by observing the convergence behavior and correct transfer of physical symmetry of the model to identical values in the capacitance matrix. For these tests, artificial and highly symmetrical models are preferred since "real" structures contain excessive complexity to determine reasons for usually observed differences in results between different programs operating on the same input model [57]. The functionality of CAMACO has been verified by comparison with results from other programs for a variety of 2D and 3D multi-body cases.

In the following chapter different examples of capacitance calculations with increased complexity are discussed. Results are compared with values obtained from the well-established and widely used commercial program RAPHAEL<sup>TM</sup> (TMA/Avant!).

The comparison with measured values from created test structures could provide further confirmation. However, one has to be aware that the creation of perfect physical structures with known dimensions on the order of some  $10^{-7}m$  is also very complicated and that such structures have deviations e.g. in line width etc.. Alternatively, models scaled to macroscopic dimension would be feasible for precise measurements.

It shall be mentioned, that results from CAMACO/ANSYS<sup>TM</sup> can slightly depend on the meshing algorithm. This explains small differences depending on the ANSYS<sup>TM</sup> version used. Results reported below have been obtained with ANSYS<sup>TM</sup> 5.4 and 5.5. (The more recent version 5.5 is recommended since its improved performance in terms of speed, as the later given numbers for example 2 show.)

### 4.2. Example 1

One of the few problems with known analytical solution (e.g. from E. Weber: "Electromagnetic Theory" [65]) is shown in Fig. 1 and consists of two infinite long cylinders with different radii  $r_1$  and  $r_2$  in a distance  $d$  within a surrounding dielectric:

$$\frac{C}{l} = \frac{2\pi\epsilon_0\epsilon_r}{\operatorname{acosh}\left(\frac{d^2 + r_1^2 - r_2^2}{2dr_1}\right) + \operatorname{acosh}\left(\frac{d^2 - r_1^2 + r_2^2}{2dr_2}\right)} \quad (14)$$

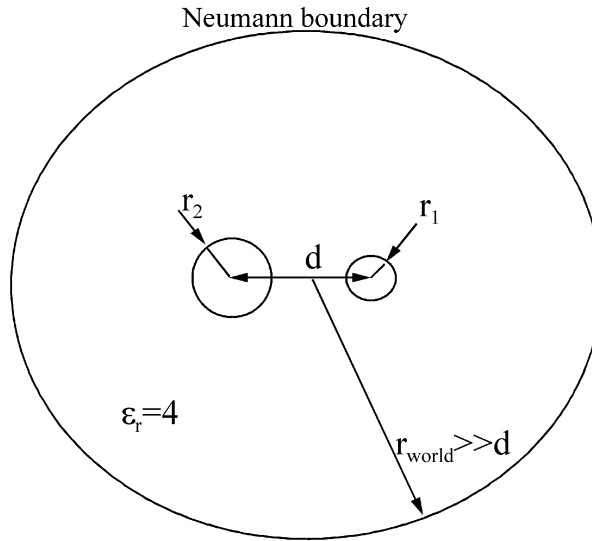


Fig. 1: Principal drawing of example 1: two infinite long cylinders with different radii  $r_1$  and  $r_2$  in a distance  $d$  within a surrounding dielectric.

For convenience the parameters are chosen as following:

- $r_1 = 0.25 \mu m$
- $r_2 = 0.15 \mu m$
- $r_{world} = 50 \mu m$
- $d = 0.66042492 \mu m$
- $\epsilon_r = 4.0$

and the expected result is  $C/l = (1 + 2 \cdot 10^{-9}) \cdot 10^{-10} F/m$ . Within RAPHAEL the simulation window was set to  $x = [-50 \mu m \dots 50 \mu m]$  and  $y = [-50 \mu m \dots 50 \mu m]$ . Calculations have been performed with CAMACO/ANSYS™ and RAPHAEL™ for different discretizations. It has been found, that for 2D-cases the removal of midside nodes (generally ANSYS™ element 121 was used) in combination with the described vector addition provides a better balance between computational effort and precision of results. Additionally, for 2-body cases it is possible to use the intrinsic EDENS function for the calculation of the field energy which provides in combination with active midside nodes about one order of magnitude improved precision. Again, this is not applicable to multi body systems unless one would sacrifice the substantial advantage of obtaining field solution by means of superposition. The results of this test are given in Fig. 2 showing the absolute amount of the relative error as function of degrees of freedom. By using Eq. (14) deviations on the order of  $|\Delta(C/C)| \approx 10^{-3}$  are obtained while by applying the EDENS-function deviations on the order of  $|\Delta(C/C)| < 10^{-4}$  can be achieved.

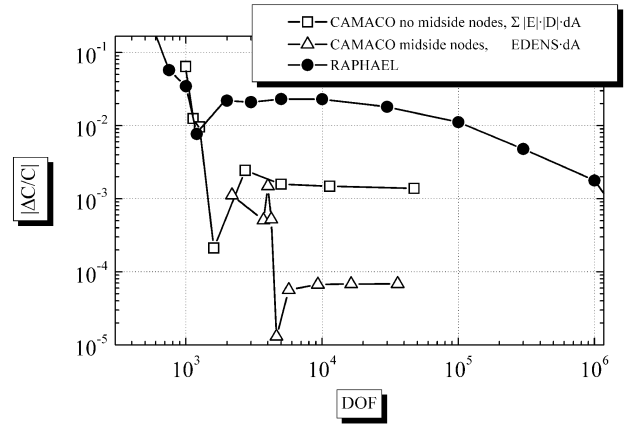


Fig. 2: CAMACO and RAPHAEL™ results for example 1: absolute value of relative error of  $C/l$  as function of DOF (number of gridpoints respectively for RAPHAEL™ results); Curve 1: CAMACO; standard use of ANSYS™ element Plane121 without midside nodes; field energy obtained from (12). Curve 2: CAMACO; maximal precision using element Plane121 with active midside nodes; field energy obtained by use of intrinsic EDENS function . Curve 3: RAPHAEL™.

#### 4.3. Example 2

This artificial example contains a structure which is more typical for cases arising from practical questions but remains still very symmetric and simple and may therefore be proposed for future references and as a simple benchmark system. It shall also serve to confirm functionality of CAMACO for multi-body problems. The example consists of 8 cubes with edge lengths of  $d = 150 nm$  each arranged at the 8 corners of a imagined cube with an edge lengths of  $d = 450 nm$  and Neumann boundaries. Consequently, a periodic continuation of the structure is imposed.

The lower and upper 4 cubes are embedded in a (cross-shaped) dielectric with  $\epsilon_r = 4$  and a flat dielectric layer with  $\epsilon_r = 2$  between the levels as illustrated in Fig. 3. This structure favors FDM approaches as e.g. used by RAPHAEL™ because of its regular shapes which especially support the mesh refinement algorithm of RAPHAEL™. Therefor a rather fast convergence of the RAPHAEL™ results could be expected.

The capacitance matrix has been calculated for the element sizes  $esize = 50 nm$  (Fig. 3, Table 2) and  $esize = 25 nm$  (Fig. 4, Table 3) with CAMACO/ANSYS™ and for  $5 \cdot 10^4$  and  $1 \cdot 10^6$  gridpoints with RAPHAEL™. The values from Table 3 and Table 5 have been used to calculate the relative deviation of the values from CAMACO and RAPHAEL™ as shown in Fig. 5.

CAMACO (by definition) and RAPHAEL™ provided very symmetric capacitance matrices which can also be seen in the symmetric appearance of the relative deviation matrices as illustrated in Fig. 5. The symmetry of the model itself (all cubes equal  $\rightarrow$  all self-capacitances equal, several equal neighbors  $\rightarrow$  only 5 different  $C_{ij}$ ) is reflected in the coefficients with errors smaller than the deviations between the results for different discretization.

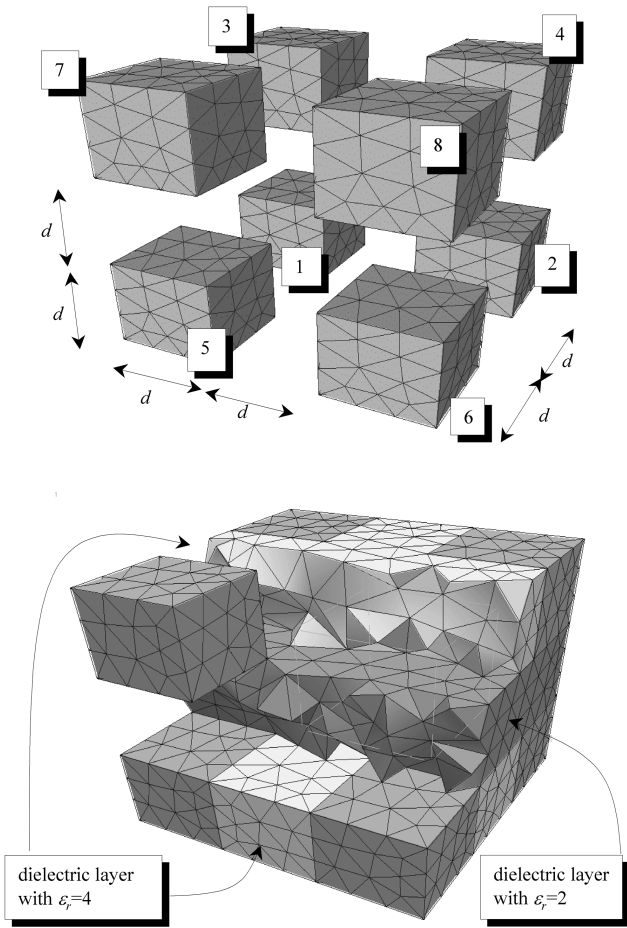


Fig. 3: Example 2: Top: eight cubes with edge lengths of  $d = 150 \text{ nm}$  arranged at the 8 corners of an imagined cube with an edge lengths of  $3d = 450 \text{ nm}$  and Neumann boundaries; Bottom: two types of dielectric layers (partially removed) fill the gaps (also cube 8 removed); meshed with  $\text{esize} = 50 \text{ nm}$ .

For  $5 \cdot 10^4$  gridpoints the RAPHAEL<sup>TM</sup> results correspond to CAMACO results on the order of  $|\Delta C_{ij}/C_{ij}| \leq 1 \cdot 10^{-2}$  and for  $10^6$  gridpoints the results are identical within  $|\Delta C_{ij}/C_{ij}| \leq 6 \cdot 10^{-3}$ . As expected this is caused by the very "Manhattan-like" structure which supports the FDM approach. On the other hand it is remarkable that the FEM approach of CAMACO/ANSYS<sup>TM</sup> gives with an  $\text{esize} = 50$

Table 2: Capacitance matrix for example 2, results from CAMACO with  $\text{esize} = 50 \text{ nm}$  as shown in Fig. 3,  $C_{ij}$  [F]; 8889 nodes, estimated number of active DOF = 5329.  $t_{CPU} = 554 \text{ s}$ ,  $t_{total} = 574 \text{ s}$  with ANSYS<sup>TM</sup> Version 5.4.  $t_{CPU} = 281 \text{ s}$ ,  $t_{total} = 345 \text{ s}$  with ANSYS<sup>TM</sup> Version 5.5.

i \ j	1	2	3	4	5	6	7	8
1	1.892E-17	-6.227E-18	-6.228E-18	-1.234E-18	-3.470E-18	-7.471E-19	-7.474E-19	-2.666E-19
2	-6.227E-18	1.893E-17	-1.235E-18	-6.235E-18	-7.480E-19	-3.473E-18	-2.661E-19	-7.455E-19
3	-6.228E-18	-1.235E-18	1.893E-17	-6.229E-18	-7.485E-19	-2.660E-19	-3.472E-18	-7.477E-19
4	-1.234E-18	-6.235E-18	-6.229E-18	1.893E-17	-2.654E-19	-7.486E-19	-7.473E-19	-3.472E-18
5	-3.470E-18	-7.480E-19	-7.485E-19	-2.654E-19	1.893E-17	-6.231E-18	-6.229E-18	-1.234E-18
6	-7.471E-19	-3.473E-18	-2.660E-19	-7.486E-19	-6.231E-18	1.894E-17	-1.236E-18	-6.234E-18
7	-7.474E-19	-2.661E-19	-3.472E-18	-7.473E-19	-6.229E-18	-1.236E-18	1.893E-17	-6.229E-18
8	-2.666E-19	-7.455E-19	-7.477E-19	-3.472E-18	-1.234E-18	-6.234E-18	-6.229E-18	1.893E-17

$\text{nm}$  and only three elements per cube edge (Fig. 3) solutions with a precision of  $|\Delta C_{ij}/C_{ij}| \leq 2 \cdot 10^{-2}$  compared with the assumed solution for infinite spatial resolution.

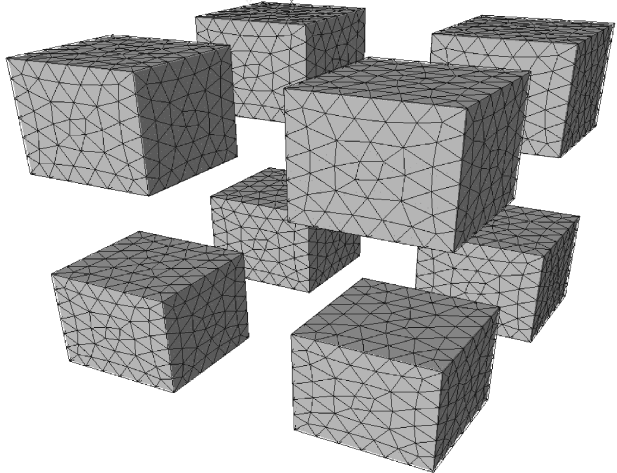


Fig. 4: The eight cubes from example 2 meshed with  $\text{esize} = 25 \text{ nm}$ .

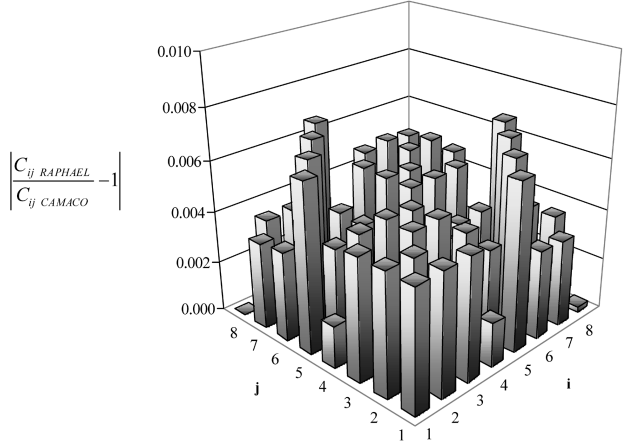


Fig. 5: Relative deviation between capacitance values  $C_{ij}$  from CAMACO with  $\text{esize} = 25 \text{ nm}$  and values from RAPHAEL<sup>TM</sup> with  $1 \cdot 10^6$  gridpoints for example 2.

Table 3: Capacitance matrix for example 2, results from CAMACO with  $e\text{size} = 25 \text{ nm}$  as shown in Fig. 4,  $C_{ij}$  [F]; 68170 nodes, estimated number of active DOF = 47032.  $t_{CPU} = 4601 \text{ s}$ ,  $t_{total} = 4735 \text{ s}$  with ANSYS<sup>TM</sup> Version 5.4.  $t_{CPU} = 1891 \text{ s}$ ,  $t_{total} = 2371 \text{ s}$  with ANSYS<sup>TM</sup> Version 5.5.

i \ j	1	2	3	4	5	6	7	8
1	1.904E-17	-6.283E-18	-6.283E-18	-1.223E-18	-3.502E-18	-7.442E-19	-7.443E-19	-2.616E-19
2	-6.283E-18	1.904E-17	-1.223E-18	-6.284E-18	-7.441E-19	-3.502E-18	-2.616E-19	-7.442E-19
3	-6.283E-18	-1.223E-18	1.904E-17	-6.283E-18	-7.441E-19	-2.616E-19	-3.501E-18	-7.442E-19
4	-1.223E-18	-6.284E-18	-6.283E-18	1.904E-17	-2.616E-19	-7.444E-19	-7.443E-19	-3.502E-18
5	-3.502E-18	-7.441E-19	-7.441E-19	-2.616E-19	1.904E-17	-6.283E-18	-6.283E-18	-1.223E-18
6	-7.442E-19	-3.502E-18	-2.616E-19	-7.444E-19	-6.283E-18	1.904E-17	-1.223E-18	-6.284E-18
7	-7.443E-19	-2.616E-19	-3.501E-18	-7.443E-19	-6.283E-18	-1.223E-18	1.904E-17	-6.283E-18
8	-2.616E-19	-7.442E-19	-7.442E-19	-3.502E-18	-1.223E-18	-6.284E-18	-6.283E-18	1.904E-17

#### 4.4. Example 3

The advantage of the FEM approach becomes apparent if instead of blocks smoothly shaped objects are used. The example consists of 6 spheres with  $r = 100 \text{ nm}$  each arranged at the three coordinate axes in a distance  $d_0 = \pm 250 \text{ nm}$  from the coordinate origin embedded in a large cube with  $V = (40 \mu\text{m})^3$ ,  $\epsilon_r = 1$  and Neumann boundaries representing the surrounding free space as shown in Fig. 6. The example is again highly symmetric providing the possibility to estimate the precision partially by means of identical values in the capacitance matrix. Only three different values are expected in this case. However, this example represents a significantly higher challenge for any FDM approach than example 2 due to the rounded surfaces.

The capacitance matrix has been calculated with the element sizes  $e\text{size} = 50 \text{ nm}$  and  $e\text{size} = 25 \text{ nm}$  on the spheres with CAMACO/ANSYS<sup>TM</sup> and for  $5 \cdot 10^4$  and  $1 \cdot 10^6$  gridpoints with RAPHAEL<sup>TM</sup>.

With  $e\text{size} = 50 \text{ nm}$ , 32385 nodes were created resulting in  $\text{DOF} = 28654$ . The computation required a CPU time of  $t_{CPU} = 496 \text{ s}$  and a total time of  $t_{total} = 676 \text{ s}$ . The results and model data for the computation with  $e\text{size} = 25 \text{ nm}$  are given in Table 6. As expected, the relative deviation between the CAMACO results from these two resolutions are  $|\Delta C_{ij}/C_{ij}| < 1.5 \cdot 10^{-2}$ . In Fig. 7 the relative deviation of values from CAMACO with  $e\text{size} = 25 \text{ nm}$  on spheres compared to values from RAPHAEL<sup>TM</sup> with  $10^6$  gridpoints are shown. Despite the high gridpoint number relative deviations up to  $|\Delta C_{ij}/C_{ij}| = 8.3 \cdot 10^{-2}$  occur.

Similar test revealed, that deviations up to  $|\Delta C_{ij}/C_{ij}| \approx 0.1$  result between FDM and FEM based codes if smooth shapes are considered, even for fine discretization. The more complex a 3D system becomes, the less precise the results are from FDM codes with given gridpoint numbers.

As an illustration of the field solutions necessary for the capacitance computation the electric field strength as contour plot in the  $[x, y]$  and  $[x, z]$  planes is shown in Fig. 8 for a given set of Dirichlet boundary conditions. The field around sphere 2 at  $[d_0, 0, 0]$  opposite to sphere 1 is relatively weak due to the shielding effect imposed by the spheres 3 through 6 and corresponding to the small capacitance coefficients for  $C_{12}$ , or

in respective cases  $C_{34}$  and  $C_{56}$ .

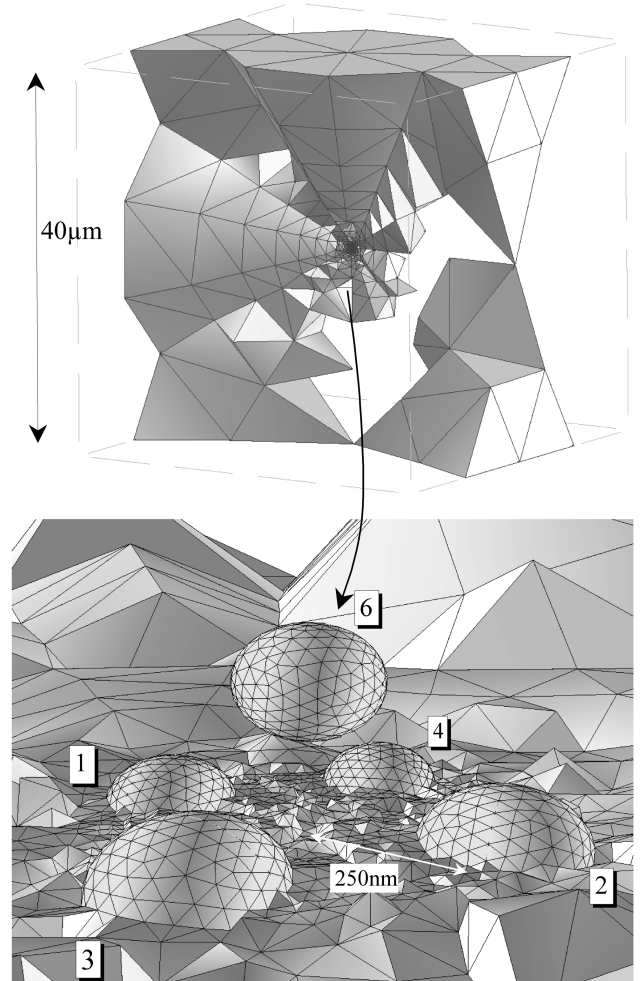


Fig. 6: Example 3: Six spheres with  $r = 100 \text{ nm}$  located at the coordinate axes at  $d_0 = \pm 250 \text{ nm}$  from the coordinate origin embedded in a cube with  $V = (40 \mu\text{m})^3$ ,  $\epsilon_r = 1$  and Neumann boundaries; Top: embedding cube, most elements removed; Bottom: enlargement, spheres meshed with  $e\text{size} = 25 \text{ nm}$  (hidden sphere 5 is opposite to sphere 6).

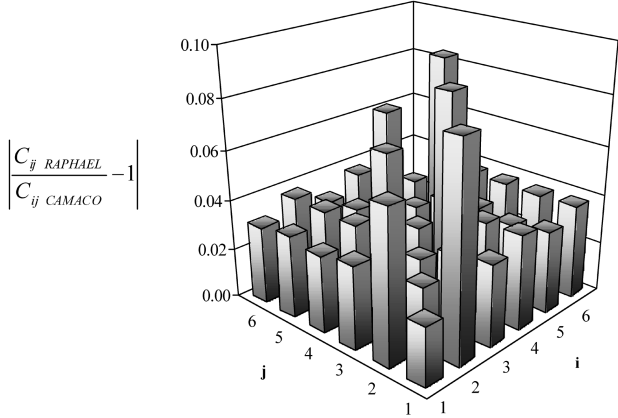


Fig. 7: Relative deviation between capacitance values  $C_{ij}$  from CAMACO with  $e\text{size} = 25 \text{ nm}$  and values from RAPHAEL<sup>TM</sup> with  $1 \cdot 10^6$  gridpoints for example 3.

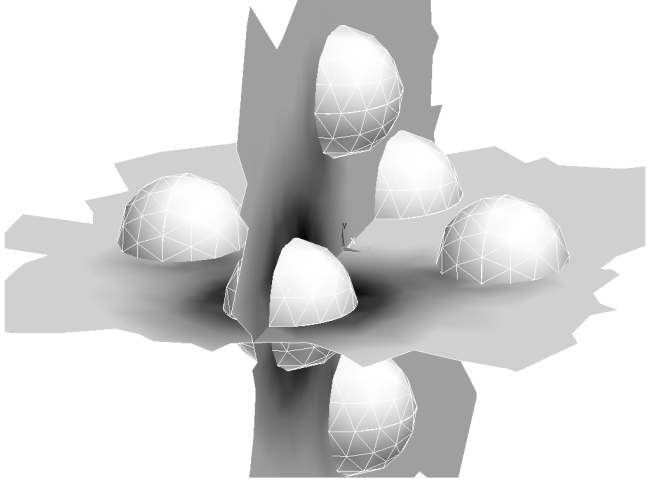


Fig. 8: Contour plot of absolute electric field strength in [x,y] and [x,z] plane for  $U = 1 \text{ V}$  applied to sphere 1 and  $U = 0 \text{ V}$  applied to sphere 2...6.

Table 4: Capacitance matrix for example 2, results from RAPHAEL<sup>TM</sup> with  $5 \cdot 10^4$  gridpoints,  $C_{ij} [\text{F}]$ .

i \ j	1	2	3	4	5	6	7	8
1	1.920E-17	-6.327E-18	-6.327E-18	-1.236E-18	-3.540E-18	-7.521E-19	-7.521E-19	-2.631E-19
2	-6.327E-18	1.920E-17	-1.236E-18	-6.327E-18	-7.522E-19	-3.540E-18	-2.634E-19	-7.522E-19
3	-6.327E-18	-1.236E-18	1.920E-17	-6.327E-18	-7.522E-19	-2.634E-19	-3.540E-18	-7.522E-19
4	-1.236E-18	-6.327E-18	-6.327E-18	1.920E-17	-2.631E-19	-7.522E-19	-7.522E-19	-3.540E-18
5	-3.540E-18	-7.521E-19	-7.521E-19	-2.630E-19	1.920E-17	-6.327E-18	-6.327E-18	-1.236E-18
6	-7.522E-19	-3.540E-18	-2.632E-19	-7.522E-19	-6.327E-18	1.920E-17	-1.236E-18	-6.327E-18
7	-7.522E-19	-2.632E-19	-3.540E-18	-7.522E-19	-6.327E-18	-1.236E-18	1.920E-17	-6.327E-18
8	-2.632E-19	-7.522E-19	-7.522E-19	-3.540E-18	-1.236E-18	-6.327E-18	-6.327E-18	1.920E-17

Table 5: Capacitance matrix for example 2, results from RAPHAEL<sup>TM</sup> with  $1 \cdot 10^6$  gridpoints,  $C_{ij} [\text{F}] t_{cpu} = 2469 \text{ s}$  (RS6000/591).

i \ j	1	2	3	4	5	6	7	8
1	1.913E-17	-6.313E-18	-6.313E-18	-1.225E-18	-3.525E-18	-7.468E-19	-7.468E-19	-2.616E-1
2	-6.313E-18	1.913E-17	-1.225E-18	-6.313E-18	-7.468E-19	-3.524E-18	-2.616E-19	-7.468E-19
3	-6.313E-18	-1.225E-18	1.913E-17	-6.313E-18	-7.468E-19	-2.616E-19	-3.524E-18	-7.468E-19
4	-1.225E-18	-6.313E-18	-6.313E-18	1.913E-17	-2.616E-19	-7.468E-19	-7.468E-19	-3.524E-18
5	-3.524E-18	-7.467E-19	-7.467E-19	-2.617E-19	1.913E-17	-6.313E-18	-6.313E-18	-1.226E-18
6	-7.468E-19	-3.525E-18	-2.619E-19	-7.468E-19	-6.313E-18	1.913E-17	-1.226E-18	-6.313E-18
7	-7.468E-19	-2.619E-19	-3.525E-18	-7.468E-19	-6.313E-18	-1.226E-18	1.913E-17	-6.313E-18
8	-2.617E-19	-7.468E-19	-7.468E-19	-3.525E-18	-1.225E-18	-6.313E-18	-6.313E-18	1.913E-17

Table 6: Capacitance matrix for example 3, results from CAMACO with  $e\text{size} = 25 \text{ nm}$  as shown in Fig. 6,  $C_{ij} [\text{F}]$ ; 119327 nodes, estimated number of active DOF= 96998.  $t_{CPU} = 1940 \text{ s}$ ,  $t_{total} = 2776 \text{ s}$  with ANSYS<sup>TM</sup> Version 5.5.

i \ j	1	2	3	4	5	6
1	1.298E-17	-1.293E-18	-2.921E-18	-2.921E-18	-2.921E-18	-2.922E-18
2	-1.293E-18	1.297E-17	-2.920E-18	-2.919E-18	-2.920E-18	-2.921E-18
3	-2.921E-18	-2.920E-18	1.298E-17	-1.293E-18	-2.920E-18	-2.921E-18
4	-2.921E-18	-2.919E-18	-1.293E-18	1.298E-17	-2.921E-18	-2.921E-18
5	-2.921E-18	-2.920E-18	-2.920E-18	-2.921E-18	1.297E-17	-1.293E-18
6	-2.922E-18	-2.921E-18	-2.921E-18	-2.921E-18	-1.293E-18	1.298E-17

## 5. Application Example

One of the targeted applications for CAMACO is the computation of parasitic interconnect capacitances in DRAM cells. The constant effort to shrink cell size by means of feature size reduction as well as cell layout modifications has to be accompanied by predictions of the impact on parasitic capacitances. Most crucial in DRAM cells is the bitline capacitance determining the capacitance transfer ratio consequently limiting the maximal possible number of cells per bitline and the capability to read out information.

In Fig. 9 and Fig. 10 such an example is illustrated. Fig. 9 shows the elements representing the dielectrics of the simulation unit-cell while the elements of the considered bodies for the capacitance matrix have been removed. Furthermore these metal volumes have been reflected to enable better envisioning of the complete structure. Fig. 10 enables insight into the unit cell on word-line and bit-line level. Noteworthy are the realistic shapes of the so called bitline studs contacting through two word-lines. The capacitance components arising from these studs are of distinct importance for the total bitline capacitance.

Typical models like this consist of approximately  $5 \cdot 10^4 \dots 2 \cdot 10^5$  nodes and the capacitance matrix includes usually 8...12 bodies. Conveniently, after the interactive, partially graphic creation of the model, further automated batch runs are possible to study dependency on parameters of interest. Runtimes are on the order of 1 to 3 hours.

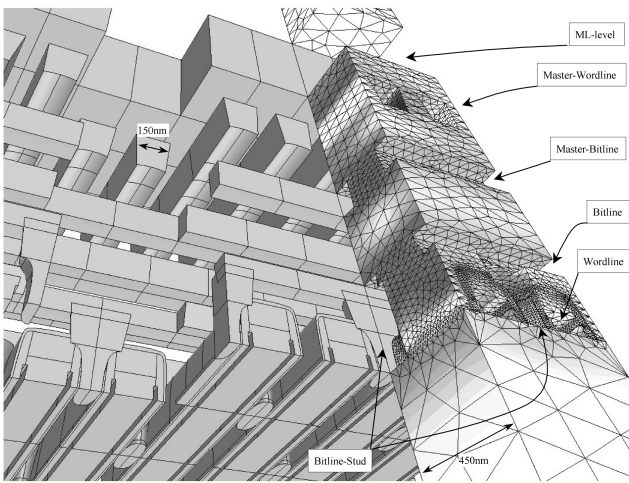


Fig. 9: Application of CAMACO/ANSYS™ in a multilevel interconnect capacitance analysis of potential trench capacitor 1 Gbit DRAM cell structure in 150 nm minimum feature size. Elements and contour plot of absolute electric field strength in dielectrics of simulation-unit cell; metals and some liner volumes repeatedly reflected; model consists of approx. 210 000 nodes, 170 000 elements; [9 × 9] capacitance matrix.

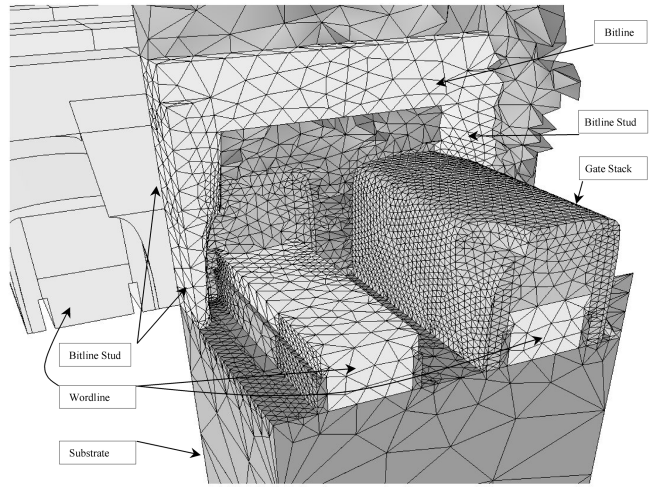


Fig. 10: Enlargement of Fig. 9: detailed view inside simulation unit-cell at wordline (WL) and bitline (BL) level; most elements of dielectrics have been removed for better visibility; notice the realistically shaped bitline-stud connecting from BL (M0-level) between two WLs to the wafer surface.

## 6. Summary

The paper described the implementation of the ANSYS Parametric Design Language macro CAMACO for the computation of capacitance matrixes of arbitrarily shaped 3D objects in arbitrarily distributed dielectrics via the conservation of field energies. The algorithm used automatically ensures the symmetry of the capacitance matrix and the correct self-capacitance values. The most significant advantage is the utilization of the advanced 3D graphics capabilities of ANSYS™ enabling interactive model generation.

The algorithm used employs the principle of energy conservation using the stored electric field energies for selected sets of boundary conditions. In addition, by taking advantage of the linear nature of the problem, field solution are obtained by superposition of solutions computed from n linear independent boundary condition vectors.

Extended investigations revealed, that it is possible achieve precision on the order of  $|\Delta C_{ij}/C_{ij}| \approx 1 \cdot 10^{-2}$  for practical problems. For 2D 2-body problems precision up to  $|\Delta C/C| < 2 \cdot 10^{-5}$  had been reached. As a real-world example the computation of parasitic interconnect capacitances in a 1 Gbit DRAM cell has been briefly discussed.

The tool provides an efficient possibility to accurately simulate capacitance matrixes of realistically shaped 3D interconnects. CAMCO is obviously not limited to the application for ULSI interconnects but can also be used for all feasible cases up to a certain degree of complexity in microsystems, MEMS, MCMs, packaging, printed boards, transmission lines or other electronic devices. CAMACO can be used on any platform running ANSYS™: AIX™, Digital Unix™, HP-UX™, IRIX™, Solaris™, UNICOS™ and WindowsNT™.

## References

- [1] Daniel Kinseth Reitan, Thomas James Higgins, "Calculation of the Electrical Capacitance of a Cube", *Journal of Applied Physics*, Vol. 22, No.2, p. 223-226, Feb. 1951
- [2] Daniel Kinseth Reitan, "Accurate Determination of the Capacitance of Rectangular Parallel-Plate Capacitors", *Journal of Applied Physics*, Vol. 30, No.2, p.172-176, Feb. 1959
- [3] Parbhubhai D. Patel, "Calculation of Capacitance Coefficients for a System of Irregular Finite Conductors on a Dielectric Sheet", *IEEE Transactions on Microwave Theory and Techniques*, Vol. 19, No.11, p. 862-869, Nov. 1971
- [4] Albert E. Ruehli, Pierce A. Brennan, "Efficient Capacitance Calculation for Three-Dimensional Multiconductor Systems", *IEEE Transactions on Microwave Theory and Techniques*, Vol. MTT-21, No.2, pp. 76-82, Feb. 1973
- [5] Peter Benedek, "Capacitance of Planar Multiconductor Configurations on a Dielectric Substrat by a Mixed Order Finite-Element Method", *IEEE Transactions on Circuits and Systems*, Vol. CAS-23, No.5, pp. 279-284, May 1976
- [6] Albert E. Ruehli, "Survey of Computer-Aided Electrical Analysis of Integrated Circuit Interconnections", *IBM Journal of Research and Development*, Vol. 23, No. 6, pp. 626-639, Nov. 1979
- [7] W. H. Dierking, J. D. Bastian, "VLSI Parasitic Capacitance Determination by Flux Tubes", *IEEE Circuits and System Magazine*, pp. 11-18, Mar. 1982[8]
- [8] Leonard T. Olson, "Application of the Finite Element Method to Determine the Electric Resistance, Inductance, Capacitance Parameters for the Circuit Package Environment", *IEEE Transactions on Components, Hybrids and Manufacturing Technology*, Vol-ChMT-5, No.4, pp. 486-492, Dec. 1982
- [9] T. Sakurai, T. Tamaru, "Simple Formulas for Two- and Three-Dimensional Capacitances", *IEEE Transactions on Electron Devices*, Vol. ED-30, No. 2, pp. 183-185, Feb. 1983
- [10] F. Straker, S. Selberherr, "Capacitance Computation for VLSI Structures", Proc. Int. Conf. Simulation of Semiconductor Devices and Processes (Swansea, UK), pp. 39-55, Jul. 1984
- [11] Sadasiva M. Rao, Tapan K. Sarkar, Roger F. Harrington, "The Electric Field of Conducting Bodies in Multiple Dielectric Media", *IEEE Transactions on Microwave Theory and Techniques*, Vol. MTT-32, No. 11, pp. 1441-1448, Nov. 1984
- [12] Peter E. Cottrell, Edward M. Buturla, "VLSI wiring capacitance", *IBM Journal of Research and Development*, Vol. 29, No. 3, pp. 277-288, May 1985
- [13] Jayanti Venkataraman, Sadasiva M. Rao, Tapan K. Sarkar, Yang Naiheng, "Analysis of Arbitrarily Oriented Microstrip Transmission Lines in Arbitrarily Shaped Dielectric Media over a Finite Ground Plane", *IEEE Transactions on Microwave Theory and Techniques*, Vol. MTT-33, No. 11", pp. 952-959, Oct. 1985
- [14] Clayborne D. Taylor, George N. ElkHouri, Thomas E. Wade, "On the Parasitic Capacitances of Multilevel Parallel Metallization Lines", *IEEE Transactions on Electron Devices*, Vol. ED-32, No. 11, pp. 2408-2414, Nov. 1985
- [15] Zhen-Qiu Ning, Patrick M. Dewildw, Fred L. Neerhoff, "Capacitance Coefficients for VLSI Multilevel Metallization Lines", *IEEE Transactions on Electron Devices*, Vol. ED-34, No. 3, pp. 644-649, Mar. 1987
- [16] Albert Seidl, Helmut Klose, Milos Svoboda, Joachim Oberndorfer, Wolfgang Rösner, "CAPCAL- A 3D Capacitance Solver for Support of CAD Systems", *IEEE Transactions on Computer-Aided Design*, Vol. 7, No.5 , pp. 549-556, May 1988
- [17] A. H. Zemanin, "A Finite-Difference Procedure for the Exterior Problem Inherent in Capacitance Computations for VLSI Interconnections", *IEEE Transactions on Electron Devices*, Vol. 35, No. 7, p. 985-991, Jul. 1988
- [18] C. S. Chang, "Electrical design of signals lines for multilayer printed circuit boards", *IBM Journal of Research and Development*, Vol. 32, No. 5, pp. 647-657, Sep. 1988
- [19] Wim Delbare, Daniel de Zutter, "Space-Domain Green's Function Approach to the Capacitance Calculation of Multiconductor Lines in Multilayered Dielectrics with Improved Surface Charge Modeling", *IEEE Transactions on Microwave Theory and Techniques*, Vol. 37, No. 10, pp. 1562-1568, Oct. 1989
- [20] A. H. Zemanian, Reginald P. Tewarson, Chi Ping Ju, Juif Frank Jen, "Three-Dimensional Capacitance Computations for VLSI/ULSI Interconnections", *IEEE Transactions on Computer-Aided Design*, Vol. 8, No. 12, pp. 1319-1325, Dec. 1989
- [21] Keith Nabors, Jacob White, "FastCap: A Multipole Accelerated 3-D Capacitance Extraction Program", *IEEE Transactions on Computer-Aided Design*, Vol. 10, No 11, pp. 1447-1459, Nov. 1991
- [22] George L. Matthaei, Gilbert C. Chinn, Charles H. Plott, Nadir Dagli, "A Simplified Means for Computation of Interconnect Disributed Capacitances and Inductances", *IEEE Transactions on Computer-Aided Design*, Vol. 11, No. 4, pp. 513-524, Apr. 1992
- [23] Thomas F. Hayes, John J. Barrett, "Modeling of Multi-conductor Systems for Packaging and Interconnecting High-Speed Digital IC's", *IEEE Transactions on Computer-Aided Design of Integrated Circuits and Systems*, Vol. 11, No. 4, pp. 424-431, Apr 1992
- [24] Albert E. Ruehli, Hansruedi Heeb, "Circuit Models for Three-Dimensional Geometries Including Dielectrics", *IEEE Transactions on Microwave Theory and Techniques*, Vol. 40, No. 7, pp. 1507-1516, Jul. 1992

- [25] Y. L. Le Coz, R. B. Iverson, "A stochastic algorithm for high speed capacitance extraction in integrated circuits", *Solid State Electronics*, Vol. 35, No.7, pp. 1005-1012, Jul. 1992
- [26] K. Nabors, S. Kim, J. White, "Fast Capacitance Extraction of General Three-Dimensional Structures", *IEEE Transactions on Microwave Theory and Techniques*, Vol. 40, No. 7, pp. 1496-1506, Jul. 1992
- [27] George W. Pan, Geofeng Wang, Barr K. Gilbert, "Edge Effect Enforced Boundary Element Analysis of Multilayered Transmission Lines", *IEEE Transactions on Circuits and Systems-I: Fundamental Theory and Applications*, Vol. 39, No. 11, pp. 955-963, Nov. 1992
- [28] Keith Nabors, Jacob White, "Multipole-Accelerated Capacitance Extraction Algorithms for 3-D Structures with Multiple Dielectrics", *IEEE Transactions on Circuits and Systems-I: Fundamental Theory and Applications*, Vol. 39, No. 11, pp. 946-954, Nov. 1992
- [29] Vijai K. Tripathi, Neven Orhanovic, "Time-Domain Characterization and Analysis of Dispersive Dissipative Interconnects", *IEEE Transactions on Circuits and Systems-I: Fundamental Theory and Applications*, Vol. 39, No. 11, pp. 938-945, Nov. 1992
- [30] Raj Mittra, W. Dale Becker, Paul H. Harms, "A General Purpose Maxwell Solver for the Extraction of Equivalent Circuits of Electronic Package Components for Circuit Simulation", *IEEE Transactions on Circuits and Systems-I: Fundamental Theory and Applications*, Vol. 39, No. 11, pp. 964-973, Nov. 1992
- [31] Hansruedi Heeb, Albert E. Ruehli, "Three-Dimensional Interconnect Analysis Using Partial Element Equivalent Circuits", *IEEE Transactions on Circuits and Systems-I: Fundamental Theory and Applications*, Vol. 39, No. 11, pp. 974-982, Nov. 1992
- [32] Peter J. Wright, Yung-Che Albert Shih, "Capacitance of Top Leads Metals-Comparison Between Formula, Simulation and Experiment", *IEEE Transactions on Computer-Aided Design of Integrated Circuits and Systems*, Vol. 12, No. 12, pp. 1897-1901, Dec. 1993
- [33] Ching-Chao Huang, "Two-Dimensional Capacitance Calculation in Stratified and/or Arbitrary Dielectric Media", *IEEE Transactions on Microwave Theory and Techniques*, Vol. 42, No. 3, pp. 501-504, Mar. 1994
- [34] K. Nabors, F. T. Korsmeyer, F. T. Leighton, and J. White, "Preconditioned, Adaptive, Multipole-Accelerated Iterative Methods for Three- Dimensional First-Kind Integral Equations of Potential Theory", *SIAM Journal on Scientific Computing*, Volume 15, Number 3, May 1994
- [35] Tai-Yo Chou, Zoltan J. Cendes, "Capacitance Calculation of IC Packages Using the Finite Element Method and Planes of Symmetry", *IEEE Transactions on Computer-Aided Design*, Vol. 13, No. 9, pp. 1159-1166, Sep. 1994
- [36] J. R. Phillips, J. White, "A Precorrected-FFT Method for Capacitance Extraction of Complicated 3-D Structures", *IEEE/ACM International Conference on Computer-Aided Design*, San Jose, CA, USA, pp.268-271, Nov. 1994
- [37] R. Bauer, "Numerical calculation of capacitances in three-dimensional interconnects" ("Numerische Berechnung von Kapazitäten in dreidimensionalen Verdrahtungsstrukturen"), Institut for Microelectronics, Technical University Vienna, Austria", Nov. 1994
- [38] Srinivas Devadas, Jacob K. White, "Computer-Aided Design Technology for High Performance Embedded Systems and Packaging", Semiannual Technical Report for the Period September 15, 1994 to March 30, 1995; Massachusetts Institute of Technology, Cambridge, Massachusetts, USA, Mar. 1995
- [39] Umakanta Choudhury, Alberto Sangiovanni-Vincenelli, "Automatic Generation of Analytical Models for Interconnect Capacitances", *IEEE Transactions on Computer-Aided Design of Integrated Circuits and Systems*, Vol. 14, No. 4, pp. 470-480, Apr. 1995
- [40] A. Deutsch, et. al., "Modeling and Characterisation of long on-chip interconnections for high performance microprocessors", *IBM Journal of Research and Development*, Vol. 39, No. 5, pp. 547-565, Sep. 1995
- [41] Narain D. Arora, Kartik V. Raol, Reinhard Schumann, Llinda M. Richardson, "Modeling and Extraction of Interconnect Capacitances for Multilayer VLSI Circuits", *IEEE Transactions on Computer-Aided Design of Integrated Circuits and Systems*, Vol. 15, No. 1, pp. 58-67, Jan. 1996
- [42] Narain D. Arora, Kartik V. Raol, Reinhard Schumann, Llinda M. Richardson, "Modeling and Extraction of Interconnect Capacitances for Multilayer VLSI Circuits", *IEEE Transactions on Computer-Aided Design of Integrated Circuits and Systems*, Vol. 15, No. 1, pp. 58-67, Jan. 1996
- [43] S. Y. Oh, K. Okasaki, J. Moll, O. S. Nakagawa,, K. Rahmat, N. Chang, "3D GIPER: Global Interconnect Parameter Extractor for Full-Chip Global Critical Path Analysis", *International Electron Devices Meeting 1996*, Technical Digest, San Francisco, CA, USA, pp. 615-618, Dec. 1996
- [44] M. Bächtold, J. G. Korvink, H. Baltes, "Enhanced multipole acceleration technique for the solution of large Poisson computations", *IEEE Transactions on Computer-Aided Design of Integrated Circuits and Systems*, Vol. 15, No. 12, pp. 1541-1546, Dec. 1996
- [45] Dirk Meyer, "Dreidimensionale Modellierung des Leiterbahnsystems integrierter Schaltungen aus Layout- und Technologiedaten zur Extraktion parasitaerer Kapazitäten", Diplomarbeit, Universität Hannover, Germany, Jun. 1997
- [46] J. Wang and J. White, "Fast Algorithms for Computing Electrostatic Geometric Sensitivities", *International Conference on Simulation of Semiconductor Processes and Devices*, Cambridge, MA, USA, pp. 129-132, Sep. 1997
- [47] Y. Ansel, B. Romanowicz, M. Laudon, P. Renaud and G. Schröpfer, "Capacitive detection method evaluation

- for silicon accelerometers by physical parameter extraction from finite element simulations", International Conference on Simulation of Semiconductor Processes and Devices, Cambridge, MA, USA, pp. 129-132, Sep. 1997
- [48] M. Bächtold, S. Taschini, J. G. Korvink, H. Baltes, "Automated Extraction of Capacitances and Electrostatic Forces in MEMS and ULSI Interconnects from the Mask Layout", International Electron Devices Meeting 1997 Technical Digest, WASHINGTON, D. C., Dec. 1997
- [49] M. Bächtold, M. Emmenegger, J. G. Korvink, H. Baltes, "An error indicator and automatic adaptive meshing for electrostatic boundary element simulations", IEEE Transactions on Computer-Aided Design of Integrated Circuits and Systems, Vol. 16, No. 12, pp. 1439-1446, Dec. 1997
- [50] Hsin-Ming Hou, Chin-Shown Sheen, Chin-Yuan Wu, "A Novel Modeling Technique for Efficiently Computing 3-D Capacitances of VLSI Multilevel Interconnections--BFEM", IEEE Transactions on Electron Devices, Vol. 45, NO. 1, pp. 200-205, Jan. 1998
- [51] J. W. Perry, Y. L. Le Coz, R. B. Iverson, "A Floating Random Walk Algorithm for solving Maxwell's Equations in Multilevel IC-Interconnect Structures", 15th VLSI Multilevel Interconnection Conference, pp. 312-315, Jun. 1998
- [52] Weiping Shi, Jianguo Liu, Naveen Kakani, Tiejun Yu, "A Fast Hierarchical Algorithm for 3-D Capacitance Extraction", 35th Design Automation Conference, San Francisco, CA, USA, pp. 212-217, Jun. 1998
- [53] E. Aykut Dengi, Ronald A. Rohrer, "Boundary Element Method Macromodels for 2-D Hierarchical Capacitance Extraction", 35th Design Automation Conference, San Francisco, CA, USA, pp. 218-223, Jun. 1998
- [54] Jinsong Zhao, Sharad Kapur, David E. Long, Wayne W.M. Dai, "Efficient Three-Dimensional Extraction Based on Static and Full-Wave Layered Green's Functions", 35th Design Automation Conference, San Francisco, CA, USA, pp. 224-229, Jun. 1998
- [55] J. Wang, J. Tausch and J. White, "Improved integral formulations for fast 3-D Method-of-Moments solvers", IEEE 7Th Topical Meeting on Electrical Performance of Electronic Packaging, West Point, NY, USA, pp. 273-276, Oct. 1998
- [56] Barry J. Rubin, "Canonical Package Problem Solved Using Six different Codes", IEEE 7Th Topical Meeting on Electrical Performance of Electronic Packaging, West Point, NY, USA, pp. 267-270, Oct. 1998
- [57] Andreas Hieke, "CAMACO - 3D FEM computation of mutual capacitances of arbitrarily shaped objects", SIEMENS Technical Report, R\_99\_1098\_PI, Siemens Microelectronics USA, 65p., Oct. 1998, (unpublished)
- [58] J. White, "Fast Algorithms for 3D Simulations", International Conference on Modeling and Simulation of Microsystems MSM99, San Juan, Puerto Rico, USA, pp. 1-3, Apr. 19-21, 1999
- [59] D. Cartwright, G. Csanak, D. George, R. Walker, A. Kuprat, A. Dengi and W. Grobman, "Capacitance Extraction from Complex 3D Interconnect Structures", International Conference on Modeling and Simulation of Microsystems MSM99, San Juan, Puerto Rico, USA, pp. 159-162, Apr. 19-21, 1999
- [60] Andreas Hieke, "Simple APDL Implementation of a 3D FEM Simulator for Mutual Capacitances of Arbitrarily Shaped Objects Like Interconnects", International Conference on Modeling and Simulation of Microsystems MSM99, San Juan, Puerto Rico, USA, pp. 172-176, Apr. 19-21, 1999
- [61] John D. Kraus, "Electromagnetics", McGraw-Hill Book Company, New York, NY, USA, 1953, p. 59
- [62] S. Flugge, "Handbuch der Physik", Band XVI Elektrische Felder und Wellen, Springer-Verlag, Berlin, Germany, 1958, p. 10
- [63] James M. Ham, Gordon R. Slemon, "Scientific Basis of Electrical Engineering", John Wiley & Sons, Inc., New York, NY, USA", 1961, p. 552
- [64] K. Simony, "Foundations of Electrical Engineering", Pergamon Press, New York, NY, USA, 1963, p. 265
- [65] Ernst Weber, "Electromagnetic Theory - Static Fields and Their Mapping", Dover Publications, Inc., New York, NY, USA, 1965, p. 15
- [66] William H. Hayt, Jr., "Engineering Electromanetics", 2nd Edition, McGraw-Hill Book Company, New York, NY, USA, 1967, p. 139
- [67] G. W. Carter, "The Electromagnetic Field in its Engineering Aspects", 2nd Edition, American Elsevier Publishing Company, Inc., New York, NY, USA, 1967, p. 50
- [68] Arthur F. Kip, "Fundamentals of Electricity and Magnetism", 2nd Edition, McGraw-Hill Book Company, New York, NY, USA, 1969, p. 104
- [69] Carl H. Durney, Curtis C. Johnson, "Introduction to Modern Electromagnetism" McGraw-Hill Book Company, New York, NY, USA, 1969, p. 308
- [70] Francis Weston Sears, "Electricity and Magnetism", Addison-Wesley Publishing Company Inc., Reading Massachusetts, USA, p. 196
- [71] S. J. Kowalski, "Electrotechnology" John F. Rider Publisher, Inc., New York, NY, USA, p. 64
- [72] Simon Ramo, John R. Whinnery, Theodore van Duzer, "Fields and Waves in Communication Electronics", 2nd Edition, John Wiley & Sons, Inc., New York, NY, USA, 1984, p. 252
- [73] David D. Ling, Albert E. Ruehli, "Interconnection Modeling" (Chap. 11 in: Circuit Analysis - Simulation and Design), North Holland, 1987, p. 211-253
- [74] Stanley Humphries Jr., "Field Solutions on Computers", CRC Press, Boca Raton, FL, USA", 1998
- [75] J. Oberndorfer, "User's Guide CAPCAL - The 3D-Capacitance Calculator for VLSI Purposes", Scientific

- Software Consulting and Systemanalysis, Munich, Germany, Dec. 1989
- [76] R. Bauer, "SCAP 1.2 User's Guide", Institute for Microelectronics, Technical University Vienna, Austria, Dec 1994
- [77] YOHKO Version 1.2 Documentation, Aug. 1995
- [78] RAPHAEL Interconnect Analysis Program Version 4.0 Reference Manual, TMA, Inc., Sunnyvale, CA, USA, Nov .1996
- [79] CLEVER User's Manual, Silvaco International, Santa Clara, CA, USA, Sep. 1997
- [80] ANSYS Basic Analysis Procedure Guide, Release 5.4, ANSYS, Inc., Canonsburg, PA, USA, Sep. 1997
- [81] ANSYS Commands Reference, Release 5.4, ANSYS, Inc., Canonsburg, PA, USA, Sep. 1997
- [82] ANSYS Elements Reference, Release 5.4, ANSYS, Inc., Canonsburg, PA, USA, Sep.,1997
- [83] Peter Kohnke, "ANSYS Theory Reference, Release 5.4", ANSYS, Inc., Canonsburg, PA, USA, Sep. 1997
- [84] J. G. Korvink and J. Funk, User Manual SOLIDISE-ISE, ISE TCAD Release 4.1, Part 21, ISE AG Zurich, Switzerland / Swiss Federal Institute of Technology (ETH) Zurich, 1997
- [85] RAPHAEL NES Version 1.0 Manual, TMA, Inc., Sunnyvale, CA, USA, Mar. 1997
- [86] <http://www.intel.com/design/PentiumII/QIT/index.htm>

*Received in Cambridge, MA, USA, 2<sup>nd</sup> June 1999*

*Paper 1/02766*

